Desaturation and structures relationships around drifts excavated in the well-compacted Tournemire's argillite and their impact on the hydraulic head profiles

Jean-Michel Matray, Sébastien Savoye, Justo Cabrera

Desaturation and structures relationships around drifts excavated in the well-compacted Tournemire's argillite and their impact on the hydraulic head profiles

Jean Michel Matray *, Sébastien Savoye, Justo Cabrera

IRSN, DEI/SARG – BP17- 92262 Fontenay-Aux-Roses, France

* Corresponding Author tel 33 1 58 35 99 05 mel jean-michel.matray@irsn.fr

Abstract

This study aimed to explore the relationships between the rock desaturation and the EDZ extension subsequent to the excavation of a century-old tunnel and recent drifts (1996 and 2003) at the Tournemire Underground Research Laboratory. The other objective of this work was to assess the impact of this desaturation on the hydraulic head profile measured around the tunnel. One section was selected per drift. Two boreholes were realized for each section: parallel and inclined (45°) with respect to the bedding. For each borehole, we performed on-site drill core mapping, petrophysical measurements and pneumatic and hydraulic tests by means of a Modular Mini-Packer System (MMPS) device.

Results indicate that EDZ around drifts is mainly a combination of unloading joints, mimicking the drift shape, and of desaturation cracks, parallel to the bedding. The EDZ extension around the tunnel is twice to three times that of drifts 1996 and 2003 and essentially composed of unloading joints resulting from the mechanical response of the rock. The masonery covering the tunnel walls is assumed to have protected the rock from the seasonal variations of the air humidity, thus limiting (without excluding) the formation of desaturation cracks. The EDZ extension deduced from core mapping is in agreement with that deduced from pneumatic tests with permeabilities several orders of magnitude greater than in the undisturbed zone. Degrees of saturation for the three sections range between 0.9 and 1 in the EDZ area and reach 1 in the undamaged zone. The head profile deduced from measurements recorded since 2002 indicates the occurrence of sub-atmospheric water pressures with an extension of *ca* 40m around the tunnel. We have searched to quantify the impact of the tunnel since its excavation on the degrees of saturation and the hydraulic heads. The simulation was performed by considering, as a first approach, the absence of fracturation in the EDZ area. A constant suction of -3300m, deduced from the mean annual values of relative humidity and temperature measured in the tunnel atmosphere since 2002, was applied at the tunnel wall. The degrees of saturation simulated around the tunnel are underestimated in the EDZ area and consistent to experimental data in the unfractured zone. The modelling of hydraulic heads is quite consistent to experimental values in the vertical direction and overestimated in the horizontal direction.

This study has demonstrated the role played by fracturation on the distribution of petrophysical parameters and of heads around drifts and the century-old tunnel. It has also demonstrated the necessity of coupling mechanic and hydraulic calculations by considering capillary forces.

Key words: Tournemire, argillite, permeability, EDZ, desaturation

1. Introduction

Argillaceous formations are considered in several European countries as potential repository host rocks for high-level radioactive wastes in deep geological formations. Their very low water velocity (due to a very low permeability and diffusivity and a moderately low hydraulic gradient) coupled to a large thickness (several hundreds of meters) and a high sorption capacity make these rocks potentially interesting for a repository as radionuclide transfer times should exceed several times the radionuclide half-lives. However, construction of a repository can lead to perturbations due to excavation works and the subsequent decompression of the surrounding rocks, ventilation of the underground drifts or construction of the engineered barriers. Host rock properties around structures (tunnel, drifts and niches) are likely altered during and after excavation works. Plastic deformations are especially expected in an altered zone called excavation disturbed zone (EDZ), depending on the mechanical properties, the initial stress field and excavation techniques (Bossart et al., 2002). A fracture network consisting in unloading fractures and of desaturation cracks is developed in this EDZ with hydraulic conductivities orders of magnitude higher than those of the unaltered zone. This fracture network can thus facilitate the transfer of radionuclides towards the biosphere along galleries and shafts in case of radionuclide release from waste containers and tightness default of engineered barriers. It can also modify the petrophysical properties of the claystone around the structure network. Porosity and water content are amongst the most sensitive properties due to the relaxing of constraints and to hydration/dehydratation cycles under low humidity conditions (Charpentier et al., 2003). Ventilation of the underground drifts and shafts during the construction and the operation phases can induce the partial desaturation of the rock around the drift, thus modifying its thermo hydro-mechanical properties (Mayor et al., 2005). This change in the rock properties affect a zone around excavations called Excavation disturbed Zone (EdZ) which may have an impact on the design of the potential repository (drift spacing and repository size). One of the greatest disturbance concerns the distribution of the hydraulic profiles around excavations.

To evaluate the impact of excavations, and more particularly, of desaturation on the hydraulic and petrophysical properties of a claystone, the French Institute of Radioprotection and Nuclear Safety (IRSN) has been conducting research programmes since 1991 in its underground research laboratory of Tournemire, in the Aveyron country (south of France). The Tournemire URL crosses a Toarcian argillaceous formation *via* a century-old tunnel and its adjacent drifts excavated in 1996 and in 2003. The tunnel and drifts are naturally ventilated since their excavation with mean annual relative humidity less than 100% and likely responsible of the partial desaturation of the rock (Ramambasoa, 2001, Valès et al., 2004).

This paper aims to characterize the extent of desaturation around the different structures (tunnel and drifts) of the URL and to understand the role of this desaturation on the petrophysic and hydraulic properties of the rock.

Characterization has been performed by means of 6 cored boreholes, with 2 boreholes per structure (century old tunnel, drift 1996 and drift 2003), one parallel to the bedding and the second with a dip angle of 45°down at the intersection of the drift and the ground to access the area assumed to be most fractured of the EDZ but also for assessing the time and structure-shape dependency on desaturation. For each drift and tunnel, these boreholes have been analyzed for their structures (unloading and tectonic joints), petrophysical properties (total porosity, gravimetric water content, degree of saturation and volumetric moisture content). In parallel, each of these boreholes has been tested for determining their permeabilities by means of pneumatic and hydraulic tests.

The role of this desaturation on the petrophysical and hydraulic properties of rock around structures is then assessed by comparing the hydraulic heads estimated around the tunnel after in situ pressure measurements to hydraulic heads obtained from a numerical simulation performed since the tunnel excavation. This preliminary modelling was performed without taking into account mechanical aspects, by means of VS2DT 3.0, a computer program developed by the U.S. Geological Survey for solving problems of water flow and solute transport in variably saturated porous media.

2. Geological, structural and hydrogeological background

The Tournemire URL is located in a Mesozoic marine basin on the southern border of the French *Massif Central* and at the western limit of the *Causse du Larzac*. The studied argillaceous formation is a 250m-thick and corresponds to sub-horizontal-indurated argillaceous and marly layer of Toarcian and Domerian age (Fig. 1). This formation is sandwiched between two carbonated and karstified aquifers.

The Tournemire *massif* is a monocline structure with a mean dip angle of about –4° to the North. The lower (Hettangian to Carixian series) and upper (Aalenian to Bathonian series) aquifers are 300m and 250m thick, respectively and essentially composed of limestone and dolomite. The argillaceous formation is composed of 250m of well-compacted and thinly bedded claystones and marls. The clay fraction is ranging between 20 and 50% of the bulk rock. It is mainly composed of illite (5 to 15%), illite/smectite mixed-layer minerals (5 to 10% with a smectitic proportion of about 10%), chlorite (1 to 5%) and kaolinite (15-20%). The claystone also contains 10 to 20% of quartz grains, 10 to 40% of carbonates (mainly composed of calcite with traces of dolomite and siderite) and 2 to 7% of pyrite (Cabrera et al., 2001; Savoye et al., 2001; Savoye et al., 2006).

The upper Toarcian is crossed by a 1885m long and century-old railway tunnel excavated between 1882 and 1886. This tunnel was an excellent opportunity to IPSN (now IRSN) to have an easy access to an argillaceous formation and develop its own research programmes for training its experts in evaluating the possibilities and processes of radionuclide transport in such kind of rocks.

The Tournemire massif is separated by a reverse and very transmissive major structure namely the Cernon fault (80km long). This fault is oriented West-East and enables the communication between the two aquifers. The massif is also affected by secondary faults of hectometric extension and oriented NW to SE. These fractures are generally filled with calcite and give access to unfractured blocks in argillites characterized by hydraulic conductivities amongst the smallest in the world (between 10^{-14} and 10^{-15} m/s *i.e.* 10^{-21} and 10^{-22} m^2 as intrinsic permeabilities) for a storativity of *ca* 10^{-6} (Boisson et al., 1998; Cabrera et al., 2001). Secondary faults sometimes present geodic cavities in relay zones that enable the vertical transfer of fluids. With the Cernon fault, these fractures are the only opportunity of getting fluids in contact with the clay formation. Hydraulic test performed on these relay structures have supplied relatively high transmissivities (around 10^{-10} m^2/s) *i.e.* with permeabilities orders of magnitude higher than those of the unfractured zone and for an equivalent tested height (Savoye et al., 2003). Fig. 2

shows the distribution of the stabilized hydraulic heads with respect to boreholes CA and DC located in the tunnel axis. Pressures have been measured in the unfractured zone with permanent sealed probes (boreholes PH1 and PH3) and a multipacker system (borehole PH2) and in the water-bearing fractures by means of double packer devices (boreholes TN2, M2 and ID180). Fig. 2 shows a depression of *ca* 30m around the tunnel with respect to the hydrostatic profile drawn from heads measured in the two aquifers (H_{CA} = 583m NGF and H_{DC}= 453m NGF). This region is characterized by the occurrence of sub-atmospheric water pressures and constitutes a capillary fringe (Horseman et al., 1996) around the tunnel as a consequence of its excavation and natural ventilation. On the contrary, the hydraulic head measured in a 80m height test section in the lower part of the argillaceous formation and isolating a water-bearing fracture likely indicates the occurrence of an overpressure in the argillite.

Two other fracture networks exist at the Tournemire URL that may have an important role on water flow and transport of dissolved species. These networks are essentially confined around the tunnel and drifts. The first one is due to the stress redistribution during excavation and subsequent rock convergence. It consists in a combination of unloading joints and fractures namely excavation disturbed zone (EDZ). The second network is made of subhorizontal fractures at the drift wall and developed parallel to the bedding (several meters deep each with a millimetric aperture and a frequency of about 1 per 10cm). This network is directly linked to seasonal variations of the drifts atmosphere (hygrometry and temperature) and attributed to variations in the chemical potential of the interstitial solutions under swelling/shrinking cycles (Ramambasoa, 2001, Valès et al., 2004). Indeed, the drift hygrometry recorded since 1999 indicates seasonal variations (40% RH and 8°C in winter and 100% and 14°C in summer) with a mean annual RH value of 77% leading to a partial evaporation of the interstitial water. There is a clear correlation between this network aperture and hygrometry with a lag time of about 60h between the fracture aperture recorded by means of extensometers and RH variations measured with capacitive thermohygrometers (Fatmi et al., 2004).

3. Materials and Methods

3.1 Realization of boreholes

Six boreholes with length ranging between 1 and 6 meters were air-drilled between June 2004 and February 2005 from the tunnel and the experimental drifts excavated in 1996 and 2003. Boreholes were realized with an Hilti device and supplied core samples of about 35 cm long each with a diameter of 55mm. Boreholes locations are shown in Fig. 3 and their main characteristics summarized in Table 1.

3.2 Drill core mapping

The core analysis and pictures were performed immediately after their removal from boreholes and just before the plug preparation for petrophysical measurements. A thorough structural analysis reported on core unrolling was performed trying to distinguish between fracturation related to the excavation works and the subsequent desaturation to that induced by tectonic events.

3.3 Petrophysical measurements by water content and volume determinations

Immediately after, the cores were entirely sawed on-site in plugs 3-4cm long each for their 105/150°C-water content and volume measurements with the goal of determining the following parameters: total porosity, volumetric moisture content, gravimetric water content and degree of saturation as a function of the distance from the borehole head. The total mass of the humid samples (M_{tot}) was measured right after sawing. Then, the total apparent volume of the humid samples (V_{tot}) was determined following the method detailed in Monnier et al. (1973) that uses Archimedes'principle by weighing the displacement of petroleum (kerdane) with a Sartorius YDK 01 density measurement kit. This determination has required i) to saturate sample in petroleum just after the M_{tot} measurement, ii) the determination of the relationship between the kerdane density and temperature iii) plus additional measurements among which the mass of humid sample in the air after saturation in oil (W_a) and the sample mass after immersion in petroleum (W_p). The plugs were then oven dried at 105°C and 150°C until stabilization (*i.e.* after 2 to 4 days for each temperature) for measuring their respective masses $M_{105°}$, $M_{150°}$. All masses were determined on-site with the same accurate scale (OHAUS, type Adventurer AR3130 having a repeatability of 0.001g for masses ranging between 0 and 310g). The grain density (ρ_s) was obtained by He-pycnometry with a mean value of 2.704 g.cm^{-3} at 105°C and 2.703 g.cm^{-3} at 150°C for a standard deviation of 0.004 g.cm^{-3}. The water density (ρ_W) was calculated from an estimation of the interstitial water to 1.0012 g.cm^{-3} with a standard deviation of 0.0004 g.cm^{-3}. The definitions of functions are those reported in Pearson et al. (2003). The total or physical porosity (n_{tot}, dimensionless) is the ratio of the pore volume to total apparent volume ($n_{tot} = V_{pores} / V_{tot}$ with $V_{pores} = V_{tot} - V_{solids} = V_{tot} - M_{105°/150°} / \rho_{s105°/150°}$ where $\rho_{s105°/150°}$ is the grain density obtained at 105°C or 150°C). The gravimetric water content, dry mass basis ($WC_{dry,105or150°}$, dimensionless) is the ratio of the mass of water ($M_W = M_{tot} - M_{105°}$ where M_{tot} represents the total mass of the humid sample) and the oven dry mass $M_{105°}$ or M_{150} such as $WC_{dry,105or150°} = 100 \times (M_w / M_{105or150°})$. The degree of saturation (S, dimensionless) is the ratio of water-filled to total pore space ($S = (V_W / V_{pores})$ with $V_w = (M_{tot} - M_{105/150°}) / \rho_W$). The volumetric moisture content (θ, dimensionless) is the ratio of water-filled pore space to total volume (V_w/V_{tot}) and becomes a function of the degree of saturation (S) and of total porosity such as: $\theta = Sr \times n_{tot}$.

In addition, there was some SEM observations performed at IRSN for verification of the occurrence or absence of heavy minerals like pyrite and lighter minerals like carbonates which have an important impact on the grain density of samples.

Errors on functions U = F(V1, V2, ...) were estimated by propagation of the analytical errors variances following the classical Gauss formula ($\sigma_U^2 = \sigma_{V1}^2 \left(\partial F / \partial V\right)^2 + \sigma_{V2}^2 \left(\partial F / \partial V\right)^2 + \ldots$ *in* Theoria combinationis, 1821).

3.4 Pneumatic and hydraulic tests

The MMPS (Modular Mini-Packer System) equipment was initially designed for hydraulic testing in the excavation disturbed zone of the Mont Terri Laboratory (Cottour et al., 1999). It allows up to five individual packer modules with a diameter of 52 mm to be coupled in a variety of configurations. Each packer module consists in a stand-alone unit with a packer inflation line and both flow and pressure measurement lines. Packer pressures are controlled by a manometer installed at the control unit, while both a manometer and a pressure transducer control interval pressures. The configuration of the MMPS is shown in the Fig. 4. A series of four 10.5 cm intervals separated through four 10 cm packers were applied. Beyond, a 100 cm packer and a last 10 cm packer located at the bottom of the MMPS were installed such that a fifth 10.5-cm interval (Fig. 4) allows a less disturbed zone to be simultaneously characterized. Use of 1-m length extension tubes permit an area up to 5m (in the tunnel boreholes) to be investigated. Pneumatic tests were performed prior to hydraulic testing to provide an estimate of both the extent and the connectivity of the fracture network and also semi-quantitative estimates of interval permeability of the tested intervals.

Pneumatic testing

Pneumatic tests have already been performed in consolidated argillaceous rocks in the Mont Terri's URL with the aim of characterizing the EDZ extension (Bossart et al., 2002). They consist in injecting nitrogen or pumping air in/out of the interval and in interpretating the corresponding pneumatic response with the MMPS device. The surface test equipment allows working with injection and extraction flow rates between 0.1 and 50 l/min at standard conditions.

The MMPS was set into the boreholes immediately after their realization. Packers were inflated to 20 to 25 bars to limit the possibility of packer bypass. Afterwards, during the injection of nitrogen or the extraction of air using a vacuum pump, the air flow rates and the pressures in the test and observation intervals were recorded with a data acquisition system. A test was stopped when steady-state conditions were either reached or the pressure and flow rate measurements indicated a permeability below the detection limit of about 5×10^{-17} m^2. The detection limit was reached when flow rates dropped below the measurement limit during air extraction tests or when pressures during injection tests were completely dominated by wellbore storage effects. The estimate of gas permeability was deduced from a steady state approximation of pneumatic test data as described in details by Bossart et al. (2002).

Hydraulic testing

They were performed right after pneumatic testing either in intervals showing values of gas permeability under the detection limit, thus indicating that rock should be water-saturated without occurrence of connected fractures, or in intervals crossing a very transmissive single fracture to verify estimates from pneumatic tests as in borehole MD6. In the former case, intervals were just filled with synthetic water and pulse-tests were applied. In the second case, the single fracture was first artificially saturated by means of a circulation of synthetic water. Then, a hydraulic cross-hole test was performed by injecting water at a constant overpressure of approximately 2m.

The pulse test data were analyzed using the method developed by Bredehoeft and Papadopoulos (1980) and the constant head injection test using a straight line analysis (Jacob and Lohman, 1952) on a pressure *vs* log time plot (see Bossart et al., 2002 for details).

4. Results

All data are shown for each section in Fig. 5 to Fig. 7 as a function of the distance from the borehole head. Each figure reports results obtained on the two boreholes of a same section (A for drift 2003, B for drift 1996 and C for the century-old tunnel). For each borehole, are given the drillcore mapping showing the extension of the EDZ, the degree of saturation calculated from petrophysical measurements of sample volumes and masses for samples oven dried at 150°C and permeabilities determined from pneumatic and hydraulic tests. The average petrophysical properties determined inside and outside the EDZ areas are summarized in Table 2.

4.1 Section A (drift 2003)

The drillcore mapping shows a destructured (DZ) Excavation Disturbed Zone (EDZ) with an extension of about 30cm and 50cm in MD2 (horizontal) and MD4 (inclined), respectively. Those destructured zones are characterized by a High Density Fracturation (HDF) combining unloading joints (UJ), mimicking the gallery shape, and desaturation cracks (DC), parallel to the bedding. Borehole MD2 also shows the occurrence of isolated unloading joints at distances of about 40 and 70cm and of a water-bearing mechanical fracture (MF) capturing water from fractures of tectonic origin. One calcite-filled microfracture of tectonic origin is also observed in MD4.
Table 1 shows that petrophysical parameters inside the EDZ are systematically lower than outside. Both boreholes show a desaturation trend in the destructured zones with values increasing from 95% in MD4 and 98% in MD2 at the borehole head up to about 100% close to the EDZ outer border with an error of ca 3%. Outside the EDZ, the rock may be considered as fully saturated. There are also two kinds of artefacts. The first one is artificial and refers to strong desaturation trends at the

core limits as a consequence of an overheating during the *in situ* core break and removal. The second type is natural and attributed to the presence or default of heavy minerals like pyrite (density of 5). Degrees of saturation greater than one as shown in MD4 are attributed to the second type after SEM observations.

The permeability profiles obtained from pneumatic tests show a progressive decrease of values which are very high (≥ 10^{-12} m^2) in the EDZ areas to very low values (≤10^{-17} m^2) in the undisturbed zones. The extent of the partially-saturated zone is greater for MD2 than for MD4 and is explained by the presence of unloading joints up to about 70cm from the borehole border in MD2. Hydraulic tests performed in the water-bearing fracture crossed in MD2 indicate a permeability of *ca* 10^{-14} m^2.

4.2 Section B (drift 1996)

There is a bigger EDZ extension in MD3 (horizontal) than in MD5 (inclined). This result is due by a bigger extension of desaturation cracks reaching *ca* 45cm and 30cm in MD3 and MD5, respectively. On the contrary, the EDZ unloading joints are limited to the very first 20cm in MD3 with a high density fracturation and reach up to 35cm in MD5 with a low density fracturation. Both boreholes also show the occurrence of tectonic microfractures filled with calcite.

As in section A, the mean values of petrophysical parameters (Table 2) are systematically lower inside the EDZ than outside. There is no clear desaturation trend in MD3 but values as low as 94% are calculated up to about 80cm. On the contrary, borehole MD5 shows a clear desaturation profile limited to the EDZ extent. In both boreholes the border artefacts are observed as in section A.

The permeability profile obtained from pneumatic tests performed in MD3 shows a progressive decrease of values from ≥ 10^{-11} m^2 in the very first 60cm down to ≤10^{-17} m^2 at about 2m, *i.e.* far away from the EDZ extension. The presence of tectonic fractures filled with calcite could explain this behaviour. Permeabilities obtained in MD5 are much more lower (10^{-16}< k m^2 < 10^{-15}) than for MD3. This behaviour is quite similar to that observed in the inclined borehole MD4 from section A. An hydraulic tests was performed in the saturated area at 2.3m from the borehole head and gave a permeability of about 10^{-18} m^2, *i.e.* very close to that determined from pneumatic tests at the same distance (10^{-17} m^2).

4.2 Section C (century-old tunnel)

The drillcore mapping shows an EDZ of about 1m in both MD6 (horizontal) and MD7 (inclined). High density fracturation of unloading joints concerns the whole EDZ in MD6 and only the first 50cm in MD7. The EDZ unloading joints observed in MD7 also show the occurrence of gypsum spots.

Table 2 shows that the MD6 petrophysical parameters are systematically lower inside the EDZ than outside. MD7 shows the inverse situation but uncertainties calculated for this borehole are so important that the real behavior may be overwhelmed by errors.

The permeability profiles obtained from pneumatic tests performed in MD6 and MD7 show very high permeabilities in the High Density Fracturation zones with values ranging between 10^{-13} and 10^{-12} m^2. An attempt of artificial saturation of this zone has allowed the conduction of an hydraulic test giving a permeability estimation of about 10^{-11} m^2, *i.e.* very close to those estimated from pneumatic tests. Permeabilities calculated out of these areas are less 10^{-17} m^2.

5. Discussion

5.1 EDZ and desaturation extensions

The study of the fracture network from the drillcore mapping shows that the extension of the EDZ at the Tournemire URL is a combination of unloading joints and of desaturation cracks. This extension is bigger around the tunnel (*ca* 1m in both boreholes MD6 and MD7) than around drift 1996 (up to 45cm from the horizontal MD3 and 30cm from the inclined MD5) which in turn shows a bigger extension than around drift 2003 (around 30 cm in the horizontal borehole MD2 and up to 40cm in the inclined MD4). Desaturation cracks are not visible around the tunnel contrary to drifts. The masonery made of limestone blocks (70-80cm thick) and covering the tunnel wall since the end of excavation works is likely protecting the rock from the natural ventilation of the tunnel and could therefore explain the lack of desaturation cracks around the tunnel. The uncovered drifts show the occurrence of desaturation cracks with a bigger extension in horizontal boreholes (MD3 and MD2) than in the inclined one (MD4 and MD5) as a consequence of cracks developed along the subhorizontal bedding planes. The extension of unloading joints decreases with the age of the structure (tunnel, drifts) and is generally bigger in inclined boreholes compared to the horizontal one. Therefore, a time-dependency on the EDZ unloading joints extension is suggested.

The permeability profiles determined from pneumatic and hydraulic tests perfectly fit the EDZ extension. Permeabilities are the highest (between 10^{-11} and 10^{-12} m^2) into the High Density Fracturation and Destructured Zones of the EDZ. They progressively decrease in the Low Density fracturation area to reach the values inferior to 10^{-17} m^2 in the undisturbed zone of the EDZ.

There is also a strong correlation between the desaturated area determined from petrophysical determinations with the extension of the EDZ deduced from the coupled study of the core mapping and of permeability measurements. With the exception of borehole MD7, all petrophysical parameters determined inside the EDZ are systematically lower than outside. The degree of saturation reflects the evolution of the water content and total porosity which are clearly linked to the extent of the EDZ fracturation. Therefore, the lower porosities and water content determined in the EDZ are likely a consequence of unloading and capillary coupled forces.

5.2. Modelling of saturation profiles and hydraulic heads around the tunnel

The main objective of this preliminary modelling is to *assess* the capability of a Richard's desaturation model to reproduce both desaturation and pressure head data measured around the tunnel. In the Richard's model (de Marsily, 1986; Genty et al., 2002), both water submitted to gravity and suction forces are taken into account. The Richard's equation is solved with a finite difference formulation implemented in VS2DTI 3.0 code (Lappala et al., 1983; Hsieh et al., 1999). The fracturation observed in the EDZ is not considered here. Model input data are porosity n_{tot}, suction curves giving the relationship between saturation S_w and suction ψ expressed as a function of the pressure head h, permeability K expressed as a product of the saturated permeability K_s and the relative permeability curve K_r function of the pressure head. Expression of $S_w(h)$ and $K_r(h)$ given below, were formulated following the van Genuchten model (van Genuchten, 1980), as follows:

$$S_e = \frac{1}{(1+|\alpha h|^{\beta})^{1-\frac{1}{\beta}}}$$

$$k_r = \left\{1-|\alpha h|^{(\beta-1)}(1+|\alpha h|^{\beta})^{(\frac{1}{\beta}-1)}\right\}\sqrt{(1+|\alpha h|^{\beta})^{(\frac{1}{\beta}-1)}}$$

Where α and β are the parameters of the van Genuchten model and S_e, the effective saturation expressed in terms of volumetric moisture content θ and residual moisture content θ_r.

$$S_e = \frac{\theta-\theta_r}{n_{tot}-\theta_r}$$

Lab and *in situ* hydraulic tests have allowed an estimate of a mean value for permeability of about 10^{-14} m.s^{-1} (Boisson et al., 2001; Bertrand et al., 2002). Parameters for the van Genuchten suction curve were deduced from lab data obtained by Daupley (1997): α= 1.5.10^{-4} , β= 2.5 and θ_r =0.0056. The mean value of total porosity measured in this study was equal to 9% (Table 2).

As the purpose of the calculations is to quantify the impact of tunnel on the saturation degrees and the hydraulic heads, the size of the simulated zone must also include domains out of the tunnel's influence. Thus, the 2D mesh consists in a 60mx120m rectangle in which a half tunnel is equidistant to the top, bottom and right side of the domain. The hydraulic boundary conditions were of the form: i) hydrostatic conditions imposed by the two surrounding aquifers were applied at the upper and lower limits; ii) a constant suction (-3300m) was imposed at the tunnel wall. The capillary pressure value was derived from the temperature and relative humidity variations (Ramambasoa, 2001; Valès et al., 2004) measured in the tunnel using the Kelvin's equation; iii) a no-flow-boundary was applied at the others limits. The initial time for simulation is the year 1888, corresponding to the end of the tunnel excavation.

Fig. 8 (a)-(b) compares the degrees of saturation simulated along boreholes MD6 and MD7 to values calculated from petrophysical data. Modelling results are roughly consistent to experimental data except in the EDZ where they are slightly lower. This discrepancy suggests that our single porosity model is likely smoothing the heterogeneities induced by the occurrence of fractures. The comparison between the simulated and the measured hydraulic heads is given in Fig. 9 (a)-(b). The modelling of hydraulic heads in the vertical direction is quite consistent with those measured in PH1 and PH3, despite the lack of in situ measurements at intermediate level. In the horizontal direction, the discrepancy between the simulated and the in situ values, especially in the deepest level, suggests that the influence of tunnel would be greater than that derived from modelling. The presence of a high density fracturation made of unloading joints resulting from the mechanical response of the rock to the present field of constraints or/and to the re-use of weakness plane of an ancient tectonic event could explain the occurrence of a capillary fringe around the tunnel. This fracturation is assumed to have increased the penetration depth of the suction effect and explains that the measured hydraulic heads are less than the simulated one. The extension of this depression may reach several tens of metres around the tunnel and makes part of the Excavation disturbed Zone (EdZ). A new modelling considering hydromechanical coupled processes is actually in progress with the aim of simulating the EDZ formation. The comparison of modellings performed in the framework of this paper to the hydromechanical coupled one will help to verify the role played by desaturation cracks on the hydraulic head profiles.

6. Conclusion

The purpose of this study was twice. Firstly, to explore the relationships between the rock desaturation subsequent to the excavation of a century-old tunnel and of modern drifts (1996 and 2003) and the EDZ extension. Secondly, to assess the impact of this desaturation on the hydraulic head profile measured around the tunnel and the drifts. One section was selected per structure (drift 2003, drift 1996 and century-old tunnel). We have realized two new boreholes for each section: one parallel to the bedding and the other one inclined downward at 45°at the gallery wall and ground intersection. For each borehole, we performed on-site drill core mapping, petrophysical measurements and at last, pneumatic and hydraulic tests by means of a Modular Mini-Packer System (MMPS) device.

Results indicate that EDZ around drifts is mainly a combination of unloading joints, mimicking the drift shape, and of desaturation cracks, parallel to the bedding. The EDZ extension around the tunnel is twice to three times that of drifts 1996 and 2003 and essentially composed of unloading joints resulting from the mechanical response of the rock to the present field of constraints or to the resumption of an ancient tectonic damage. The masonery covering the tunnel walls is assumed to have protected the rock from the seasonal variations of the air humidity, thus limiting (without excluding) the formation of desaturation cracks. The EDZ extension deduced from core mapping is also in agreement with that deduced from pneumatic tests with permeabilities several orders of magnitude greater than in the undisturbed zone. Degrees of saturation deduced from petrophysical measurements for the three sections range between 0.9 and 1 in the EDZ area and reach saturation in the undamaged zone. Hydraulic heads are measured since 2002 by permanent pressure probes installed in the unfractured rock around the tunnel and by piezometers installed in the surrounding aquifers. The head profile indicates the occurrence of sub-atmospheric water pressures with an extension of *ca* 40m around the tunnel. We have searched to quantify the impact of the tunnel since its excavation on the degrees of saturation and the hydraulic heads. The simulation was performed with the VS2DTI 3.0 code by using the Richard's desaturation model and considering, as a first approach, the absence of fracturation in the EDZ area. A constant suction of -3300m, deduced from the mean annual values of relative humidity and temperature measured in the tunnel atmosphere since 2002, was applied at the tunnel wall. The degrees of saturation simulated around the tunnel are underestimated in the EDZ area and consistent to experimental data in the unfractured zone. The modelling of hydraulic heads is quite consistent to experimental values in the vertical direction and overestimated in the horizontal direction. The occurrence of an unloading-joints fracture network resulting from the mechanical response of the rock to the present field of constraints or to the re-use of weakness zones of an ancient tectonic event is assumed to have created very high capillary pressures in the EDZ and could therefore explain discrepancies between the observed and simulated hydraulic heads.

This study has demonstrated the role played by fracturation on the distribution of petrophysical parameters and of heads around drifts and the century-old tunnel. It has also demonstrated the necessity of coupling mechanic and hydraulic calculations by considering capillary forces. Such calculations will be performed in a next step.

Acknowledgments

The authors gratefully acknowledge S. Lemius for his help when carrying out petrophysical measurements and M. Piedevache and M. Kech from Solexperts for performing pneumatic and hydraulic testing. We also wish to give our acknowledgement to C. Combes for realizing boreholes.

References

Bertrand, L., Laviguerie, R., Cabrera, J., Matray, J.-M., Savoye, S., 2002. Instrument for measuring pore pressure and permeability in low permeability rock. International meeting "Clays in natural and engineered for radioactive waste confinement", organized by ANDRA in Reims, Conference Proceeding, 321-322.

Boisson, J.Y., Cabrera, J., Bertrand L., Heitz, J.F., 1998. Mesures de très faibles perméabilités in situ et en laboratoires sur les argilites de Tournemire (Aveyron). Méthodologies comparées et effet d'échelle. Bull. Soc. Géol. France, 169, 595-604.

Boisson, J.Y., Bertrand, L., Heitz J.F., Moreau-Le Golvan, Y., 2001. In situ and laboratory investigations of fluid flow through an argillaceous formation at different scales of space and time, Tournemire tunnel, southern France. Hydrogeol. J. 9, 108-123.

Bossart, P., Meier, P.M., Moeri, A., Trick, T., Mayor, J.C., 2002. Geological and hydraulic characterisation of the excavation disturbed zone in the Opalinus Clay of the Mont Terri Rock Laboratory. Eng. Geol. 66, 19-38.

Bredehoeft, J.D., Papadopoulos, S.S., 1980. A method for determining the hydraulic properties of tight formations. Water Resour. Res. 16, 233-238.

Cabrera, J., Beaucaire, C., Bruno, G., De Windt, L. Genty, A., Ramanbasoa, N., Rejeb, A., Savoye, S., Volant, P., 2001. Projet Tournemire – Synthèse des programmes de recherche 1995-1999, Rapport IPSN DPRE/SERGD 01-19, Paris France.

Charpentier, D., Tessier, D., Cathelineau, M., 2003. Shale microstructure evolution due to tunnel excavation after 100 years and impact of tectonic paleo-fracturing. Case of Tournemire, France. Eng. Geol. 70, 55-69.

Cottour, Ph., Bigarré, P., Camus, P., Bauer-Plaindoux, C., Blümling, P.,1999. Evaluation of in-situ stresses. Comparison of techniques. In: M. Thury and P. Bossart, Editors, *Results of the Hydrogeological, Geochemical and Geotechnical Experiments, Performed in 1996 and 1997. Swiss National Geological and Hydrogeological Survey. Geological Report* vol. 23, pp. 160–170.

de Marsily, G., 1986. Quantitative hydrogeology, Academic Press inc. (London).

Daupley, X., 1997. Etude du potentiel de l'eau interstitielle d'une roche argileuse et des relations entre ses propriétés hydriques et mécaniques. Thèse de l'Evocole Nationale Supérieure des Mines de Paris.

Fatmi, H., Mangin, A., Matray, J.M., 2004. Traitement et exploitation des séries temporelles de pression, température et humidité obtenues sur le site de Tournemire. Rapport IRSN/DEI/SARG 04-24, Paris, France.

Genty, A., Bassot, S., Bruno, G., Cabrera, J., Le Potier, C., 2002. Modelling of desaturation experiments on Tournemire argillite samples. Poromechanics II, Auriault et al. (eds.), 437-443.

Horseman, S.T., Higgo, J.J.W., Alexander, J., Harrington, J.F., 1996. Water, gas and solute movement through argillaceous media. OECD/NEA CC-96/1:290.

Hsieh, P.A., Wingle, W., Healy R.W., 1999. A graphical software package for simulating fluid flow and solute or energy transport in variably saturated porous media. US. Geological Survey report- Water Resources Investigations N°99-4130.

Jacob, C.E., Lohman, S.W., 1952. Nonsteady flow to a well of constant drawdown in an extensive aquifer. Trans. AGU 33 (1952), pp. 559–569.

Lappala, E.G., Healy, R.W., Weeks, E.P., 1983. Documentation of computer program VS2D to solve the equations of fluid flow in variably saturated porous media. US. Geological Survey report- Water Resources Investigations N°83-4099.

Mayor, JC., Garcia-Sineriz, J.L., Velasco, M., Gomez-Hernandez, J., Lloret, A., Matray, J.M., Coste, F., Giraud, A., Rothfuchs, T., Marshall, P., Fierz, T., Klubertanz, G., 2005. Ventilation Experiment in Opalinus Clay for the disposal of radioactive waste in underground repositories. (Project funded by the European Communnity under the 'EURATOM' Programme 1998-2002 under contract N° FIKW-CT-2001-00126). EC Final Tech. Publ. Rept. CEC Nuclear Science & Technology Series Luxembourg pp. 41.

Monnier, G., Stengel, P., Fies, JC., 1973. Une méthode de mesure de la densité apparente de petits agglomérats terreux. Application à l'analyse de système de porosité du sol. Ann. Agron. 24, 533-545.

Pearson, F.J., Arcos, D., Bath, A., Boisson, J.Y., Fernandez, A.M., Gabler, H.E., Gaucher, E., Gautschi, A., Griffault, L., Hernan, P., Waber, H.N., 2003. Mont Terri project – Geochemistry of Water in the Opalinus Clay Formation at the Mont Terri Rock Laboratory. Rapport de l'OFEG, Série Géologie, N°5 , Bern, 319p.

Ramambasoa, N., 2001. Etude du comportement hydromécanique des argilites: Application au site de Tournemire. Thèse de l'Ecole Polytechnique.

Savoye, S., de Windt, L., Beaucaire, C., Bruno, G., Guitard, N., 2001. Are artificial tracers conservative in argillaceous media ? The Tournemire claystone case. In Cidu (Ed.), Water Rock Interaction proceedings 10, 1383-1386.

Savoye, S., Cabrera, J., Matray, J.M., 2003. Different hydraulic properties of single fractures in argillaceous medium: the case of the IRSN Tournemire site (France). IAH Conference IAH "Groundwaters in fractured rocks", Prague (Tchéquie), sept 2003, Conference Proceeding, 47-50.

Savoye, S., Michelot, J.L., Wittebroodt, C., Altinier, M.V., 2006. Contribution of the diffusive exchange method to the characterization of pore-water in consolidated argillaceous rocks. J. Contam. Hydrol., in press.

Valès, F., Nguyen Minh, D., Gharbi, H., Rejeb, A., 2004. Experimental study of the influence of the degree of saturation on physical and mechanical properties in Tournemire shale (France). Appl. Clay Sci. 26, 197-207.

van Genuchten, M.T., 1980. A closed-form equation for predicting the hydraulic conductivity of unsaturated soils. Soil Sci. Soc. Am. 44, 892-898.

Figure captions

Fig. 1. Geological cross section of the Tournemire URL.

Fig. 2. Hydraulic head profile through the argillaceous formation at Tournemire.

Fig. 3. Boreholes location and sections in the structural context of the Tournemire URL.

Fig. 4. Schematic view of the MMPS device.

Fig. 5. Drillcore mapping, gas permeability and degree of saturation as a function of the distance for boreholes MD2 and MD4 drilled from the drift 2003.

Fig. 6. Drill core mapping, gas permeability and degree of saturation as a function of the distance for boreholes MD3 and MD5 drilled from the drift 1996.

Fig. 7. Drill core mapping, gas permeability and degree of saturation as a function of the distance for boreholes MD6 and MD7 drilled from the century-old tunnel

Fig. 8. Comparison of modeled degrees of saturation with measured ones (A) in borehole MD6 and (B) in borehole MD7.

Fig. 9. Comparison of modeled hydraulic with measured ones (A) in horizontal direction and (B) in vertical direction. Only positive simulated hydraulic head values were represented in the figure for clarity reasons and all negative ones were fixed at zero.

Fig. 1

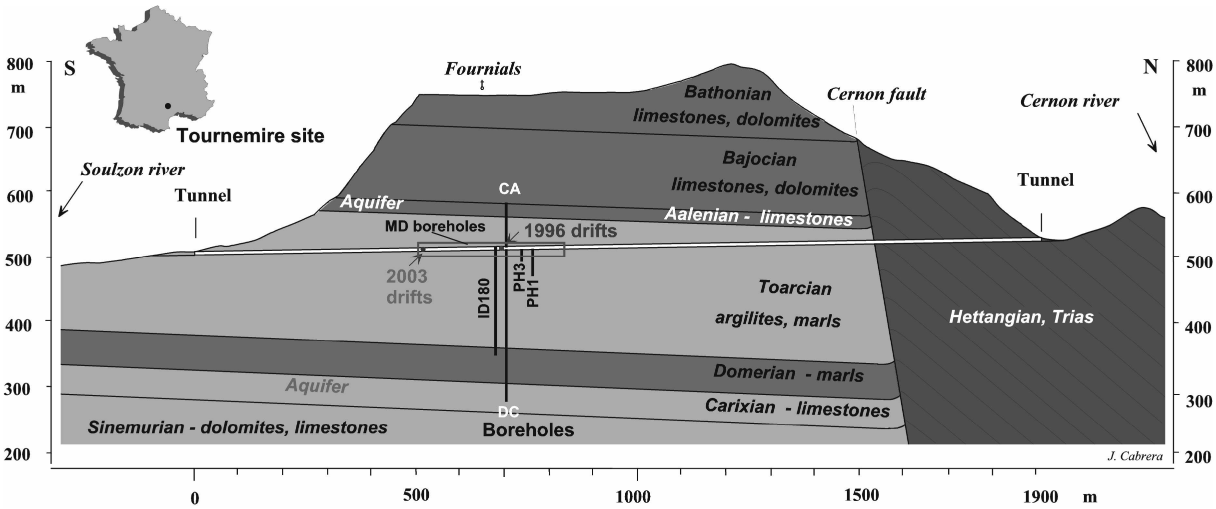

Tournemire site
S
N
800 m
700
600
500
400
300
200
Fournials
Bathonian limestones, dolomites
Cernon fault
Cernon river
Bajocian limestones, dolomites
Soulzon river
Tunnel
CA
Aquifer
Aalenian - limestones
Tunnel
MD boreholes
1996 drifts
2003 drifts
ID180
PH3
PH1
Toarcian argilites, marls
Hettangian, Trias
Domerian - marls
Aquifer
Carixian - limestones
DC
Sinemurian - dolomites, limestones
Boreholes
J. Cabrera
0
500
1000
1500
1900 m

Fig. 2

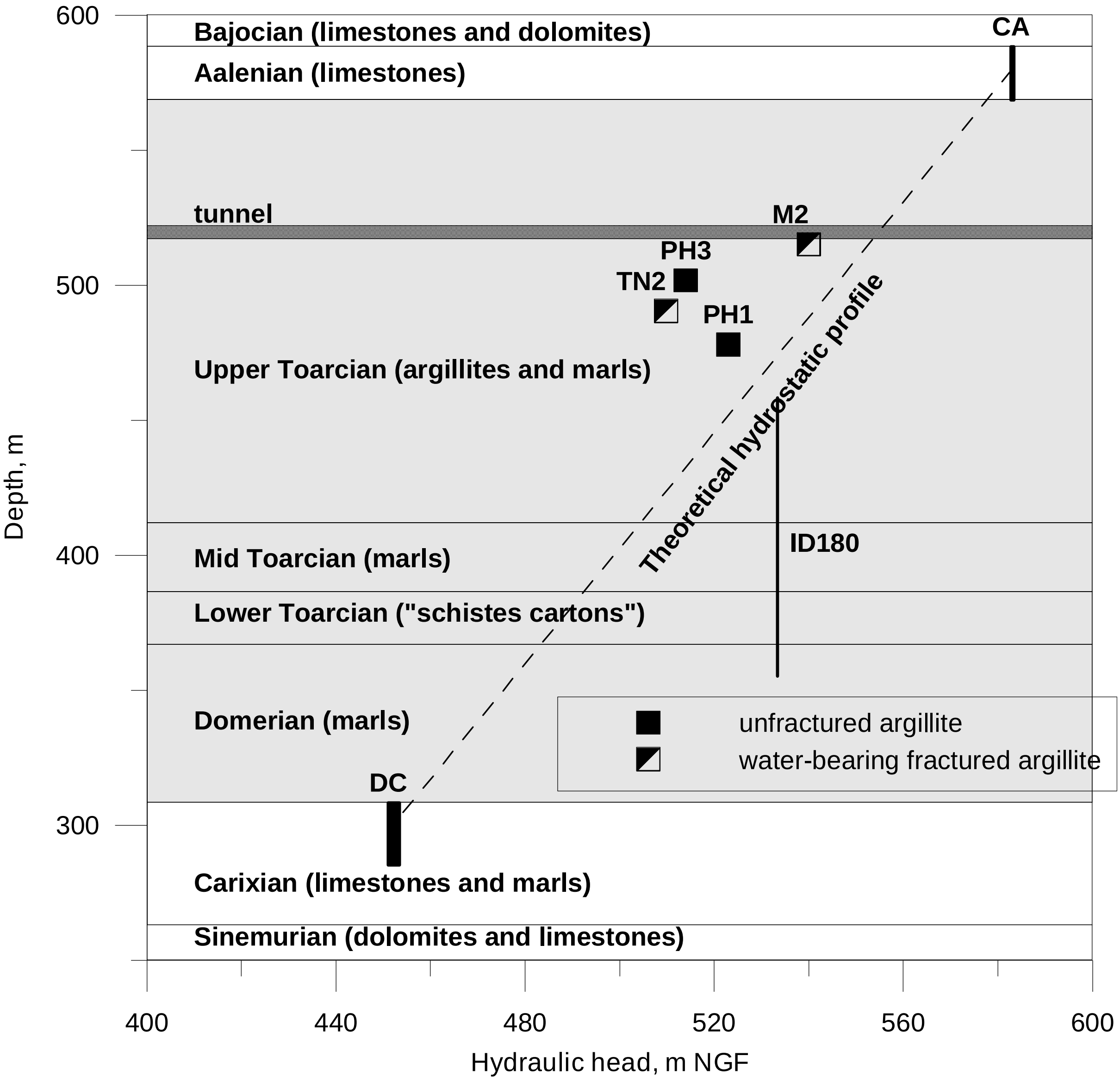
600
500
400
300
Depth, m
Bajocian (limestones and dolomites)
CA
Aalenian (limestones)
tunnel
M2
PH3
TN2
PH1
Upper Toarcian (argillites and marls)
Theoretical hydrostatic profile
ID180
Mid Toarcian (marls)
Lower Toarcian ("schistes cartons")
Domerian (marls)
unfractured argillite
water-bearing fractured argillite
DC
Carixian (limestones and marls)
Sinemurian (dolomites and limestones)
400
440
480
520
560
600
Hydraulic head, m NGF

Fig. 3

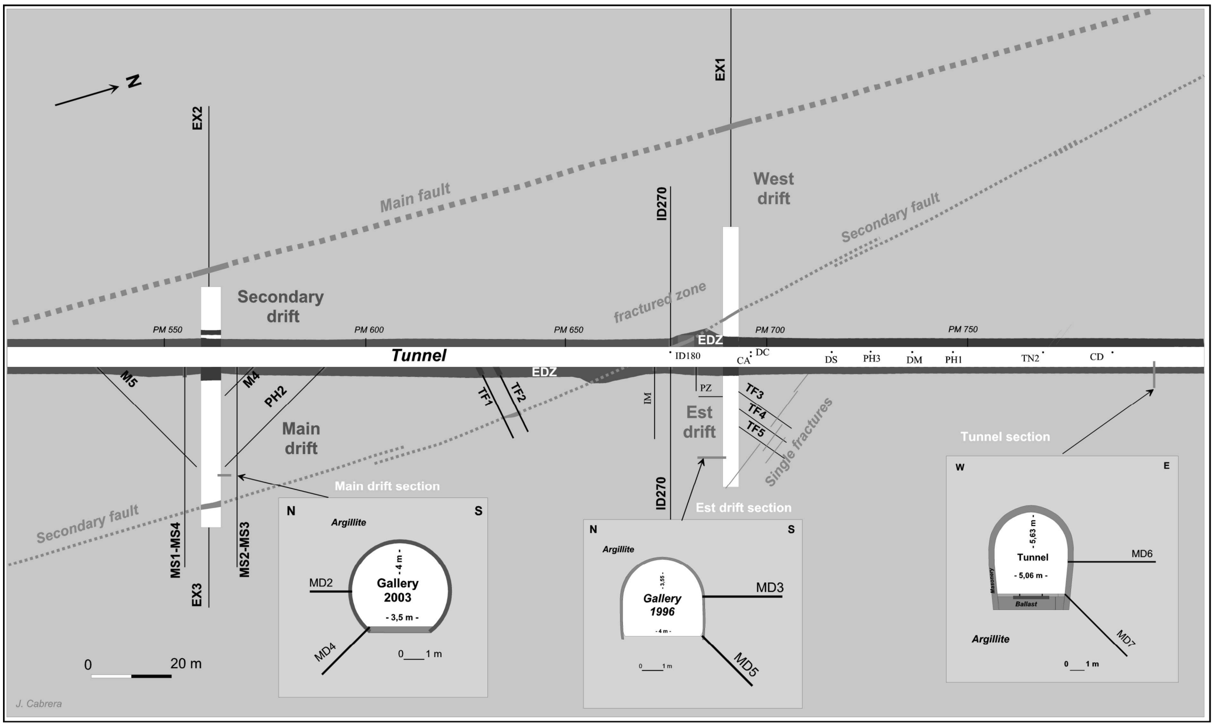
N
EX2
EX1
Main fault
West
drift
ID270
Secondary fault
Secondary
drift
fractured zone
PM 550
PM 600
PM 650
PM 700
PM 750
EDZ
Tunnel
ID180
CA
DC
DS
PH3
DM
PH1
TN2
CD
EDZ
M5
M4
PH2
TF1
TF2
IM
PZ
TF3
TF4
TF5
Est
drift
Single fractures
Main
drift
Main drift section
Tunnel section
Secondary fault
MS1-MS4
MS2-MS3
EX3
ID270
Est drift section
N
S
Argillite
MD2
Gallery
2003
- 3,5 m -
MD4
0 1 m
N
S
Argillite
Gallery
1996
MD3
MD5
W
E
Tunnel
- 5,06 m -
- 5,63 m -
MD6
Ballast
Argillite
MD7
0 1 m
0
20 m
J. Cabrera

Fig. 4

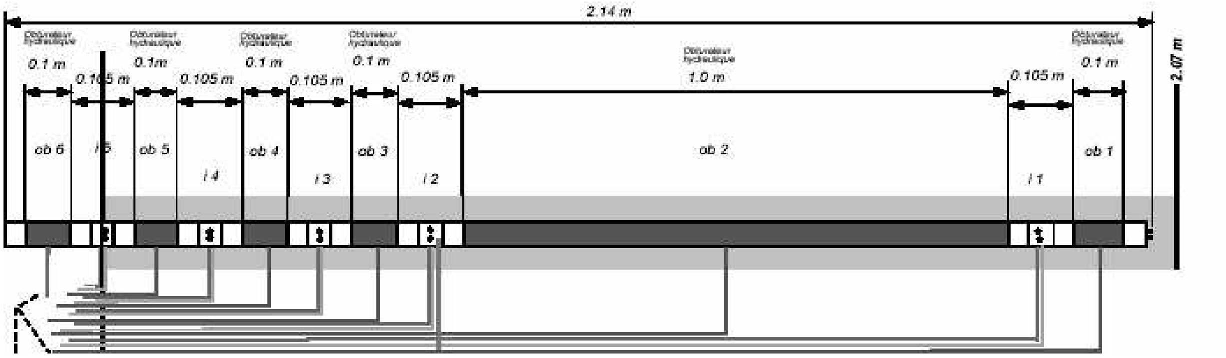

2.14 m
2.07 m
0.1 m
0.105 m
0.1m
0.105 m
0.1 m
0.105 m
0.1 m
0.105 m
1.0 m
0.105 m
0.1 m
ob 6
ob 5
i 4
ob 4
i 3
ob 3
i 2
ob 2
i 1
ob 1

Fig. 5

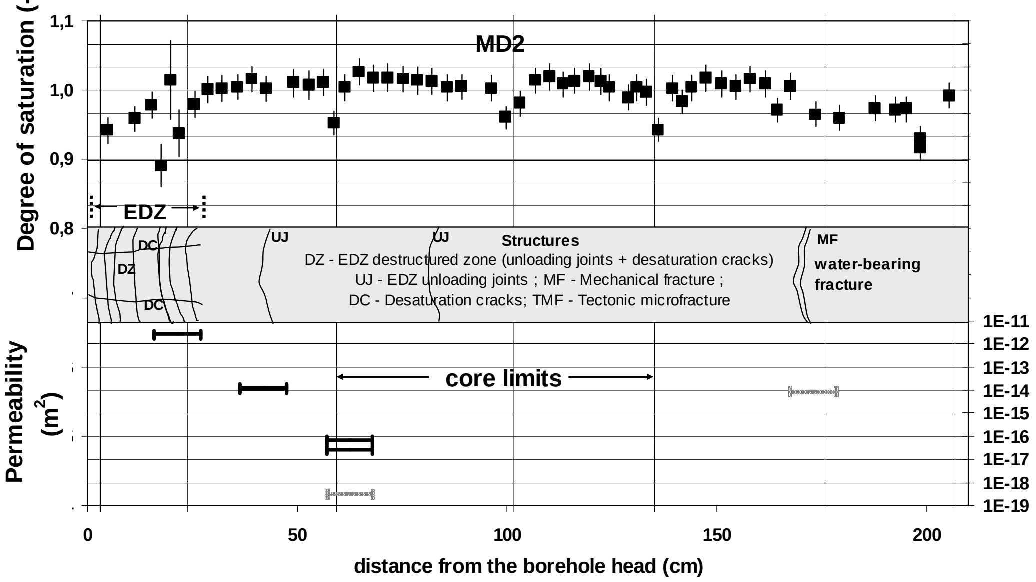
MD2
Degree of saturation (-)
1,1
1,0
0,9
0,8
EDZ
DC
DZ
DC
UJ
UJ
Structures
DZ - EDZ destructured zone (unloading joints + desaturation cracks)
UJ - EDZ unloading joints ; MF - Mechanical fracture ;
DC - Desaturation cracks; TMF - Tectonic microfracture
MF
water-bearing
fracture
Permeability
(m2)
core limits
1E-11
1E-12
1E-13
1E-14
1E-15
1E-16
1E-17
1E-18
1E-19
0
50
100
150
200
distance from the borehole head (cm)

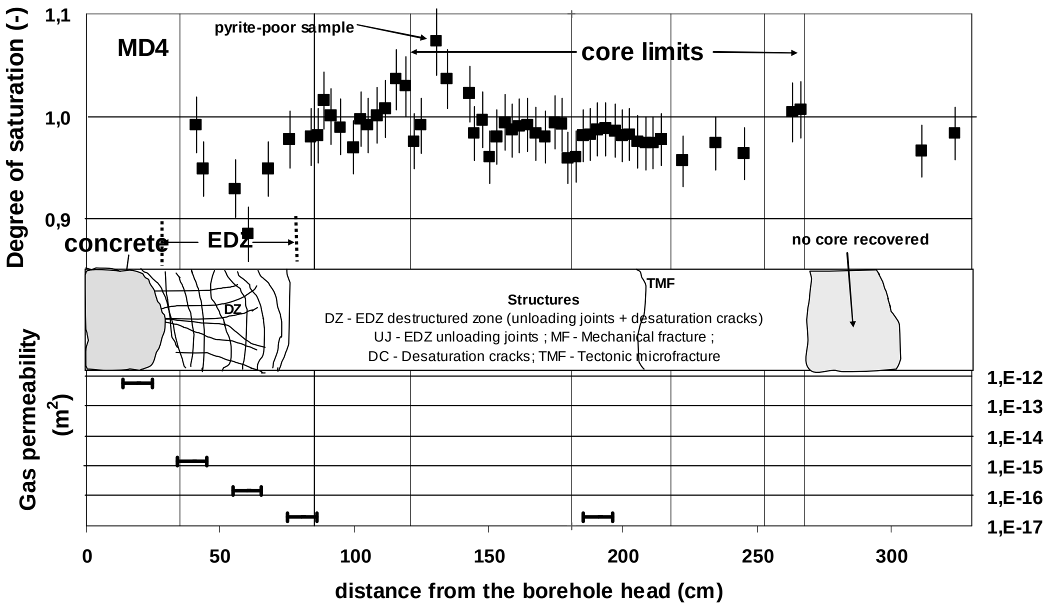
MD4
pyrite-poor sample
core limits
Degree of saturation (-)
1,1
1,0
0,9
concrete
EDZ
no core recovered
TMF
DZ
Structures
DZ - EDZ destructured zone (unloading joints + desaturation cracks)
UJ - EDZ unloading joints ; MF - Mechanical fracture ;
DC - Desaturation cracks; TMF - Tectonic microfracture
Gas permeability
(m2)
1,E-12
1,E-13
1,E-14
1,E-15
1,E-16
1,E-17
0
50
100
150
200
250
300
distance from the borehole head (cm)

Fig. 6

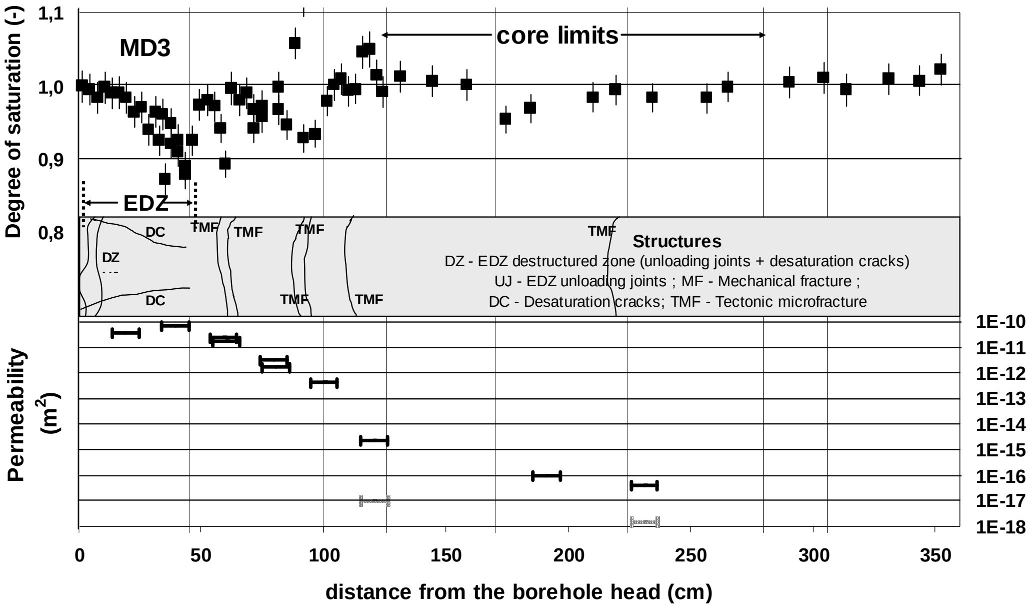
MD3
core limits
EDZ
Degree of saturation (-)
1,1
1,0
0,9
0,8
DC
DZ
TMF
Structures
DZ - EDZ destructured zone (unloading joints + desaturation cracks)
UJ - EDZ unloading joints ; MF - Mechanical fracture ;
DC - Desaturation cracks; TMF - Tectonic microfracture
Permeability (m^2)
1E-10
1E-11
1E-12
1E-13
1E-14
1E-15
1E-16
1E-17
1E-18
0
50
100
150
200
250
300
350
distance from the borehole head (cm)

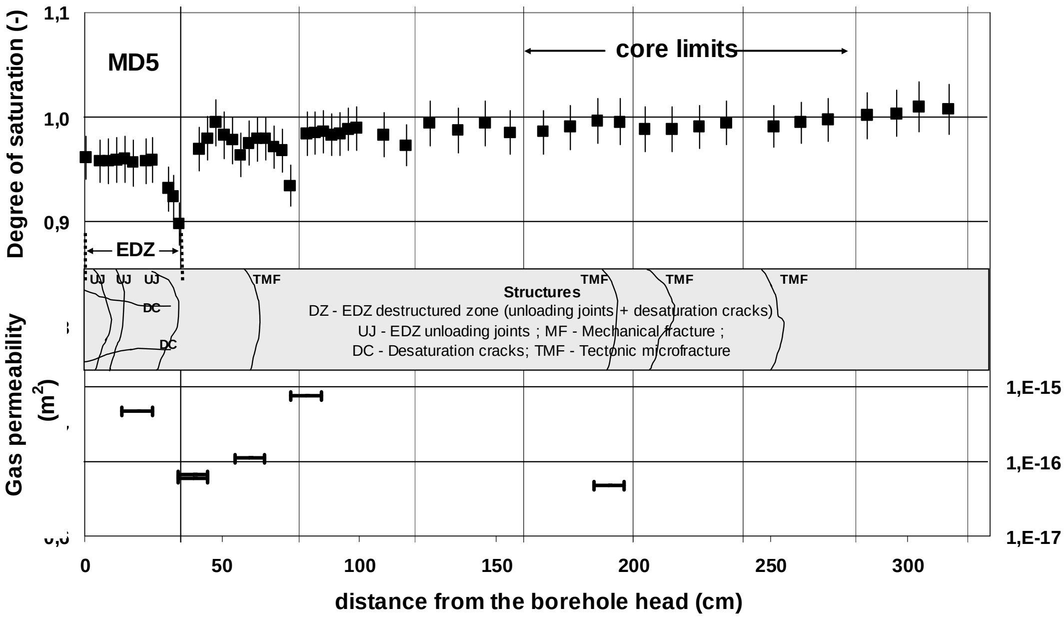
MD5
core limits
EDZ
Degree of saturation (-)
1,1
1,0
0,9
UJ
DC
TMF
Structures
DZ - EDZ destructured zone (unloading joints + desaturation cracks)
UJ - EDZ unloading joints ; MF - Mechanical fracture ;
DC - Desaturation cracks; TMF - Tectonic microfracture
Gas permeability (m^2)
1,E-15
1,E-16
1,E-17
0
50
100
150
200
250
300
distance from the borehole head (cm)

Fig. 7

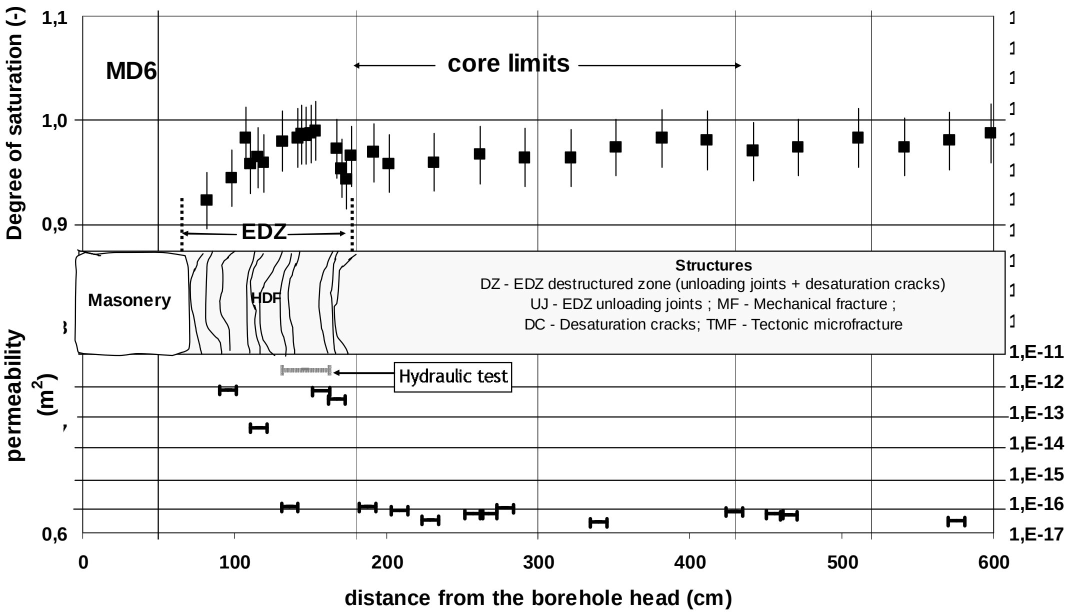

MD6
core limits
EDZ
Masonery
HDF
Structures
DZ - EDZ destructured zone (unloading joints + desaturation cracks)
UJ - EDZ unloading joints ; MF - Mechanical fracture ;
DC - Desaturation cracks; TMF - Tectonic microfracture
Hydraulic test
Degree of saturation (-)
permeability (m2)
distance from the borehole head (cm)

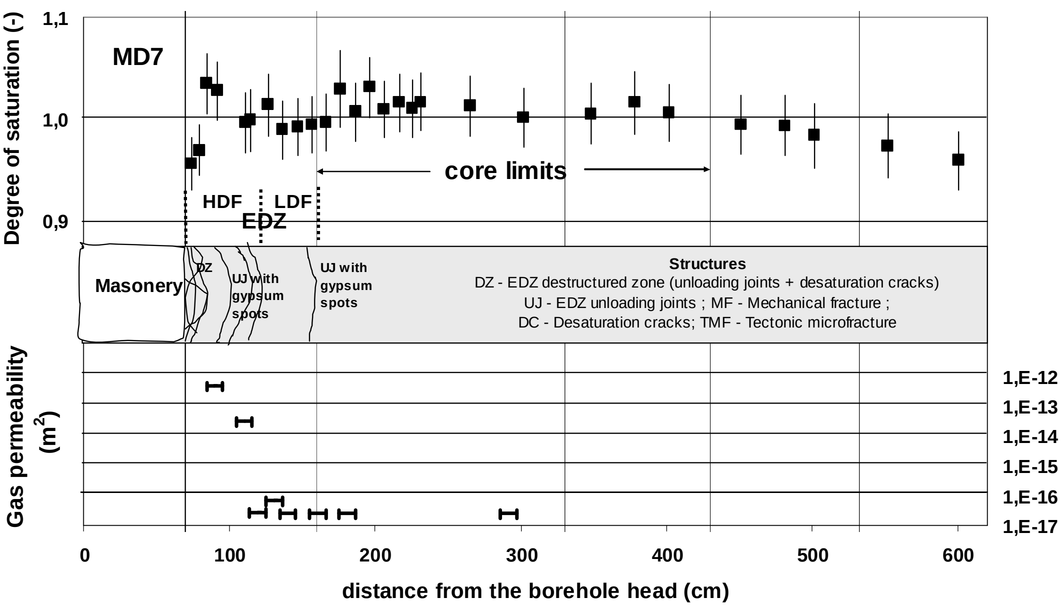

MD7
core limits
HDF
LDF
EDZ
Masonery
DZ
UJ with gypsum spots
UJ with gypsum spots
Structures
DZ - EDZ destructured zone (unloading joints + desaturation cracks)
UJ - EDZ unloading joints ; MF - Mechanical fracture ;
DC - Desaturation cracks; TMF - Tectonic microfracture
Degree of saturation (-)
Gas permeability (m2)
distance from the borehole head (cm)

Fig. 8 (A) and (B)

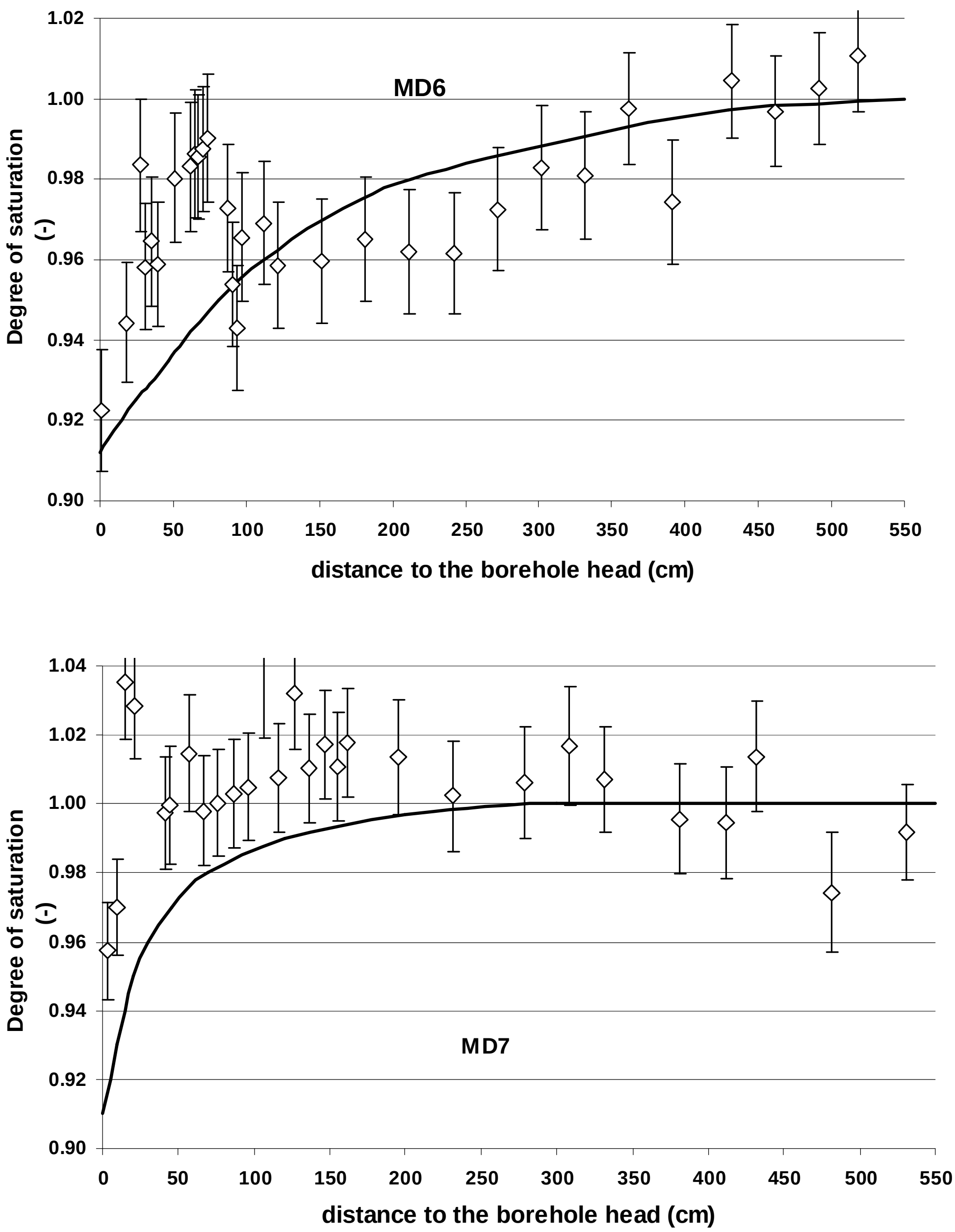

MD6
Degree of saturation (-)
1.02
1.00
0.98
0.96
0.94
0.92
0.90
0 50 100 150 200 250 300 350 400 450 500 550
distance to the borehole head (cm)
MD7
Degree of saturation (-)
1.04
1.02
1.00
0.98
0.96
0.94
0.92
0.90
0 50 100 150 200 250 300 350 400 450 500 550
distance to the borehole head (cm)

Fig. 9 (A) and (B)

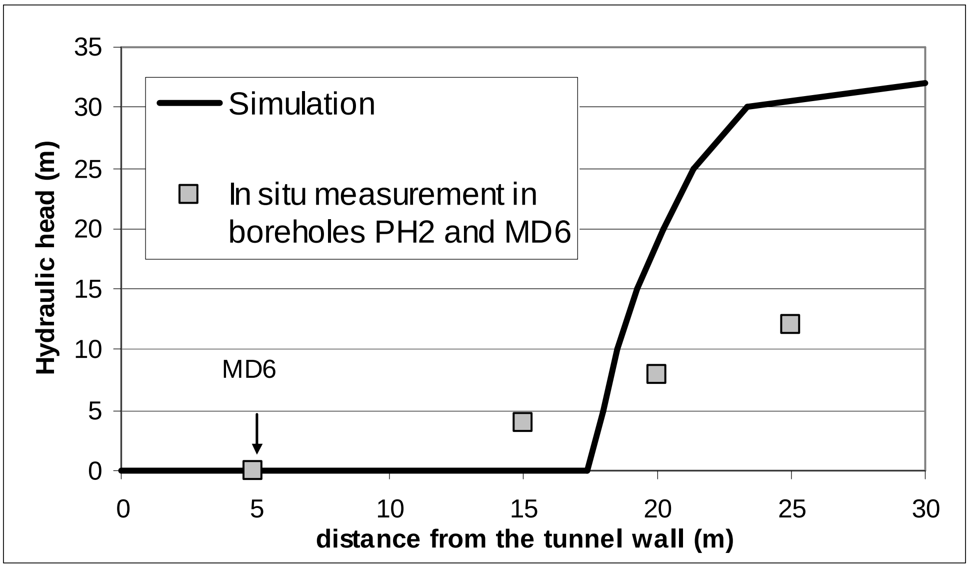

Simulation
In situ measurement in
boreholes PH2 and MD6
MD6
Hydraulic head (m)
distance from the tunnel wall (m)
0
5
10
15
20
25
30
35

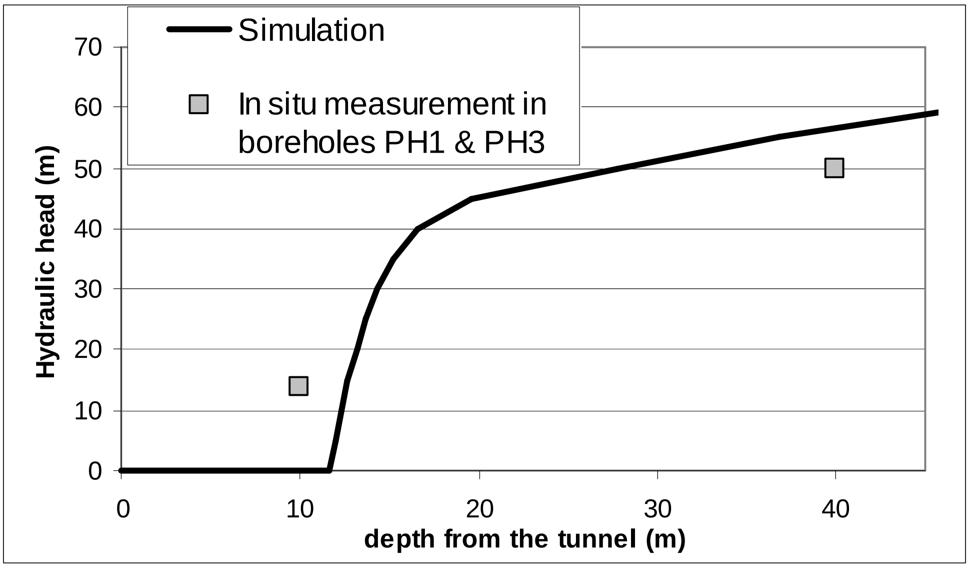

Simulation
In situ measurement in
boreholes PH1 & PH3
Hydraulic head (m)
depth from the tunnel (m)
0
10
20
30
40
50
60
70

Table 1

Main objectives (C for petrophysical measurements, H hydraulic tests, P pneumatic tests) and characteristics of boreholes realized in the framework of this study. Section A, B and C refers respectively to gallery 2003, gallery 1996 and century-old tunnel.

ID /section	Aim	Date	Drift (distance from the tunnel)	Azimuth	Dip angle	Length	Height of borehole head/ ground
					Degree	*m*	*m*
MD2 /A	C/H /P	29/06/04	Drift 2003 (27m N wall)	N15	0° sub parallel to bedding	2.07	1.6
MD3 /B	C/H /P	12/10/04	Drift 1996 (23m)	N195	0°sub parallel to bedding	3.58	1.5
MD4 /A	C/P	22/11/04	Drift 2003 (27m)	N15	45°down	3.41	1.6
MD5 /B	C/P	23/11/04	Drift 1996 (23m)	N15	45°down	3.22	1.5
MD6 /C	C/H /P	23/02/05	Tunnel 1885	N105	0°sub parallel to bedding	6.00	1.87
MD7 /C	C/P	22/02/05	Tunnel 1885	N105	45°down	6.00	1.87

Table 2

Average values of water content, total porosity, volumetric moisture content and degree of saturation determined Inside and Outside the EDZ areas.

Borehole	EDZ	$WC_{dry,150°}$, %	n_{tot}, %	θ, %	S, %
MD2	In	3.073 $\pm$ 0.003	7.79 $\pm$ 0.18	7.612 $\pm$ 0.38	97.7 $\pm$ 2.7
MD2	Out	4.085 $\pm$ 0.003	9.92 $\pm$ 0.18	9.93 $\pm$ 0.37	100.1 $\pm$ 1.8
MD3	In	3.284 $\pm$ 0.007	8.53 $\pm$ 0.18	8.14 $\pm$ 0.65	95.1 $\pm$ 2.1
MD3	Out	3.562 $\pm$ 0.005	8.87 $\pm$ 0.18	8.77 $\pm$ 0.65	98.9 $\pm$ 2.5
MD4	In	3.891 $\pm$ 0.021	9.95 $\pm$ 0.28	9.51 $\pm$ 0.64	95.2 $\pm$ 2.7
MD4	Out	4.150 $\pm$ 0.005	10.07 $\pm$ 0.27	10.06 $\pm$ 0.63	100.1 $\pm$ 2.7
MD5	In	3.180 $\pm$ 0.004	8.31 $\pm$ 0.18	7.91 $\pm$ 0.38	94.9 $\pm$ 2.1
MD5	Out	3.456 $\pm$ 0.004	8.67 $\pm$ 0.18	8.53 $\pm$ 0.37	98.6 $\pm$ 2.1
MD6	In	3.670 $\pm$ 0.003	9.29 $\pm$ 0.27	9.04 $\pm$ 0.64	96.9 $\pm$ 2.8
MD6	Out	3.704 $\pm$ 0.003	9.38 $\pm$ 0.27	9.11 $\pm$ 0.65	97.0 $\pm$ 2.8
MD7	In	3.910 $\pm$ 0.003	9.60 $\pm$ 0.27	9.57 $\pm$ 0.64	99.7 $\pm$ 2.8
MD7	Out	3.783 $\pm$ 0.004	9.26 $\pm$ 0.27	9.29 $\pm$ 0.64	100.3 $\pm$ 2.9